# CONSIDERATIONS ON LIMITS OF DREDGING PROCESSES

**S.A. Miedema**[1]

## ABSTRACT

In hydraulic dredging, two main dredging processes occur. On one hand, soil has to be excavated and on the other hand, the soil has to be transported.
When excavating soft soil, the excavating process is limited by bulldozing or clogging of the cutterhead resulting in a high-excavated production. This causes a high-density mixture to be transported hydraulically. In this case usually vacuum, pressure or sedimentation occurring in the hydraulic system limits the hydraulic transportation process. Which of these is the real limit, depends on the type of soil and on the pipeline and pump layout. When excavating hard to dig soil, the excavating process is limited by the cutter torque available. The excavated production will be low, so the hydraulic system will not give limitations.
The paper describes the different processes involved for sand cutting and transportation and gives some tools on how to determine the transition between excavating limitations and hydraulic limitations.
By means of simulations and calculations, both limitations will be illustrated.

## INTRODUCTION TO SAND CUTTING

In dredging, the excavation of soil is one of the most important processes. It is known that on the largest cutter suction dredges thousands of kW's are installed on the cutter drive. To predict the forces on excavating elements, two-dimensional cutting theories are used. Van Os 1977 [12], Verruijt 1985 [14], Miedema 1987 [6] and 1989 [7] and van Leussen & van Os 1987 [13] described the two-dimensional cutting theory for water saturated sand and its applications extensively. The aim of developing such theories is to predict the loads on excavating elements like cutter heads, drag heads, etc. It is however also possible to predict the production, when the soil mechanics parameters, the geometry of the excavating element and the available power are known. The soil mechanics parameters are described by van Leussen & Nieuwenhuis in 1984 [5].

The cutting process of a cutter head is very complicated. Not only do the blades have a three-dimensional shape; also, the velocities on the blades are three-dimensional, with respect to their direction, due to a combination of the swing velocity and the circumferential velocity. Figure 1 shows the 3D shape of a cutterhead. Other excavating elements such as dredging wheels, blades in dragheads and trenchers, may not look that complicated, but will also require the three-dimensional cutting theory to fully describe the cutting process. In 1994, Miedema [8] described the three-dimensional cutting theory.

[1]Associate Professor, Chair of Dredging Technology, Director of Education, Mechanical Engineering, Delft University of Technology.

To derive forces, torque, power, specific energy and production from the above-mentioned theories, requires complicated calculations, while the soil mechanics parameters of the sand have to be known. Mostly, only the SPT (Standard Penetration Test) value of the sand is known. In 1995 Miedema [9] described how to determine the production of a hydraulic dredge based on cutting theories for sand cutting.

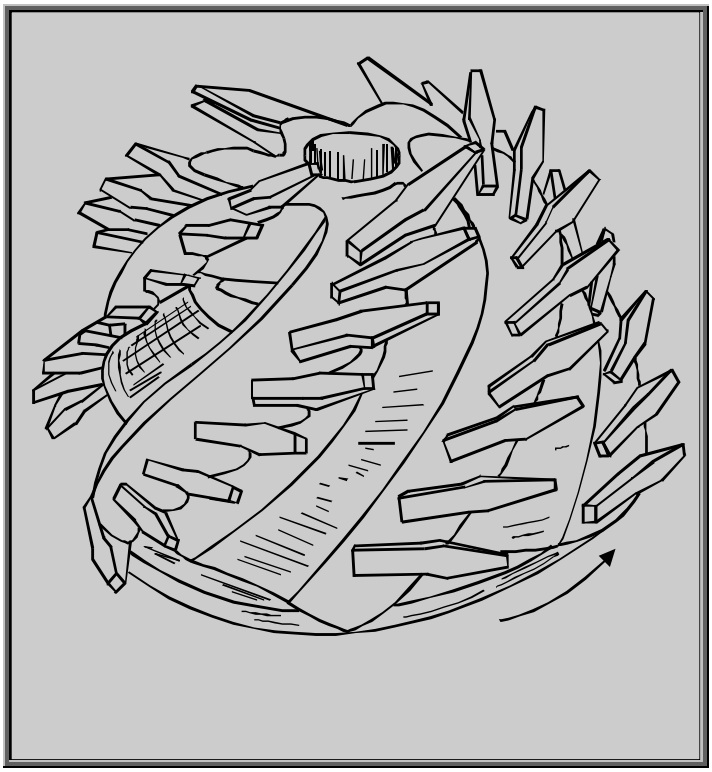

Fig. 1: The 3D shape of a cutterhead.

In 1975, Hatamura and Chijiiwa [3] distinguished three failure mechanisms in soil cutting. The "shear type", the "flow type" and the "tear type". A fourth failure mechanism can be distinguished, the "curling type", as is known in metal cutting. Although it seems that the curling of the chip cut is part of the flow of the material, whether the "curling type" or the "flow type" occurs depends on several conditions. The "flow type", "tear type" and "curling type" occur in clay, while the "tear type" and, under high hydrostatic pressure, the "flow type" occur when cutting rock. The "shear type" occurs in materials with an angle of internal friction, but without cohesion like sand. Figure 2 illustrates the four failure mechanisms as they might occur when cutting soil. Although the "shear type" is not a continuous cutting process, the shear planes occur so frequently, that a continuous process is assumed. The Mohr-Coulomb failure criteria is used to derive the cutting forces. This derivation is made under the assumption that the stresses on the shear plane and the blade are constant and equal to the average stresses acting on the surfaces.

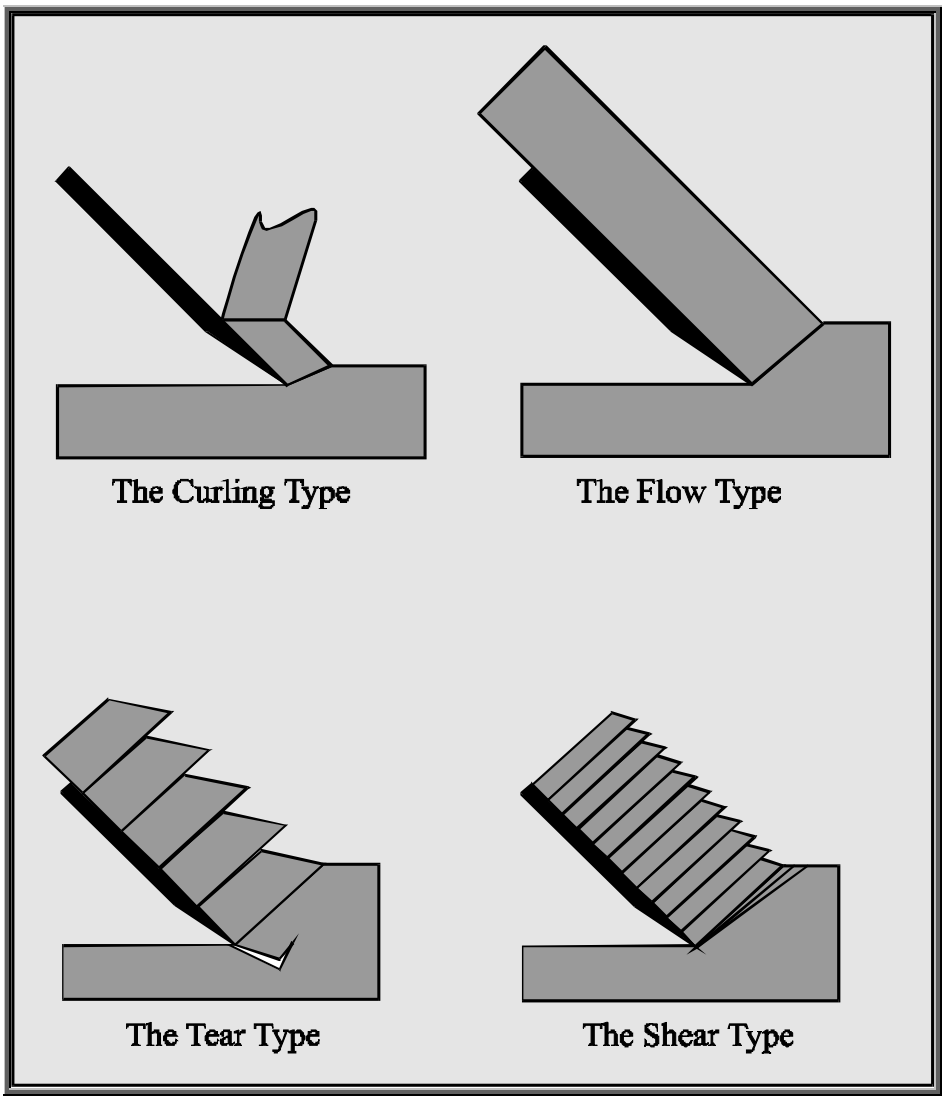

Fig. 2: Failure mechanisms in soil cutting.

## THE EQUILIBRIUM OF FORCES.

The forces acting on a straight blade when cutting soil, can be distinguished as:

1. A force normal to the blade $N_2$.
2. A shear force $S_2$ as a result of the soil/steel friction $N_2 \cdot \tan[\delta]$.
3. A shear force A as a result of pure adhesion between the soil and the blade. This force can be calculated by multiplying the adhesive shear strength of the soil with the contact area between the soil and the blade.
4. A force $W_2$ as a result of water under pressure on the blade.

These forces are shown in figure 3. If the forces $N_2$ and $S_2$ are combined to a resulting force $K_2$ and the adhesive force and the water under pressure distribution is known, then the resulting force $K_2$ is the only unknown force on the blade.

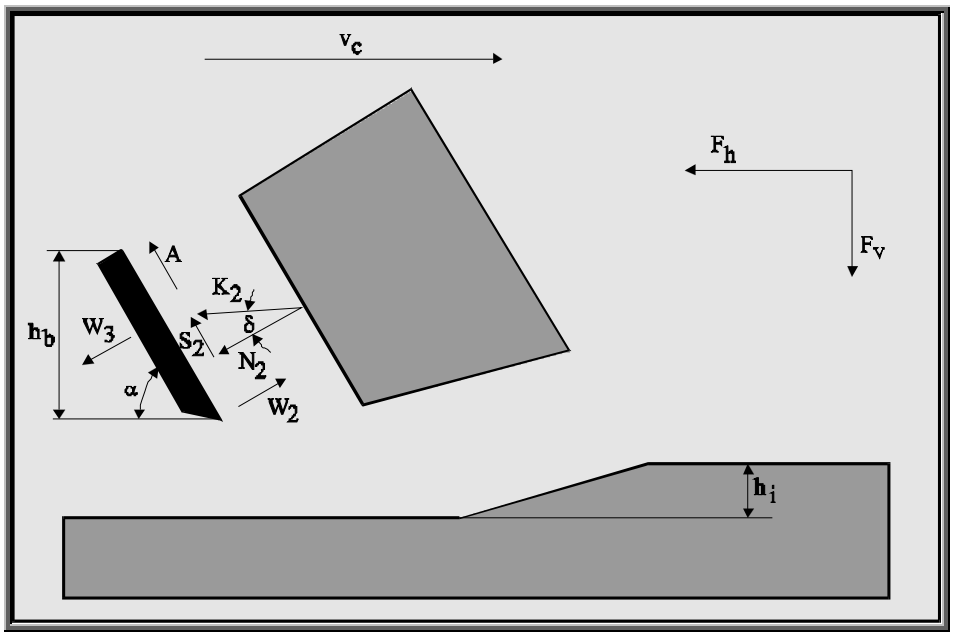

Fig. 3: The forces acting on the blade.

The forces acting on the layer cut are:

1. The forces occurring on the blade as mentioned above.
2. A normal force acting on the shear surface $N_1$.
3. A shear force $S_1$ as a result of internal fiction $N_1 \cdot \tan[\phi]$.
4. A force $W_1$ as a result of water under pressure in the shear zone.
5. A shear force C as a result of pure cohesion. This force can be calculated by multiplying the cohesive shear strength with the area of the shear plane.
6. A gravity force G as a result of the weight of the layer cut.
7. An inertial force I, resulting from acceleration of the soil.

The normal force $N_1$ and the shear force $S_1$ can be combined to a resulting grain force $K_1$. By taking the horizontal and vertical equilibrium of forces, an expression for the force $K_2$ on the blade can be derived.

Figure 4 illustrates the forces on the layer of soil cut. The forces shown are valid in general. In sand, several forces can be neglected. In fact the forces resulting from the water underpressure dominate the cutting of water saturated sand. From literature, it is known that, during the process of cutting sand, the pore volume of the sand increases. This is caused by the phenomenon dilatancy (see figure 5 and 6). With a certain cutting velocity $v_c$ there has to be a flow of water to the shear zone, the area where the pore volume increases. This causes a decrease in the pore pressure of the pore water and because the soil stress remains constant, the grain stress will increase. Van Os [12] 1977 stated: "If it is the aim of the engineer to know the average cutting forces needed to push the blade through the soil, he can take an average deformation rate $\delta e/\delta t$ to insert into the Biot equation. But it should be noted that this is purely practical reasoning and has nothing to do with Theoretical Soil Mechanics". Van Os and van Leussen

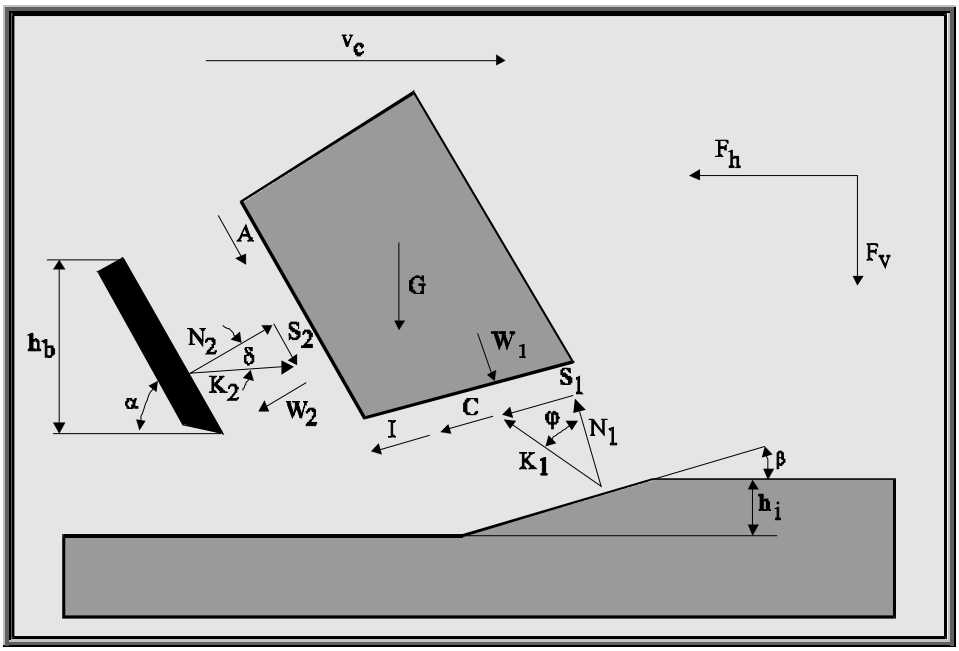

Fig. 4: The forces acting on the layer cut.

published their cutting theory in 1987 [13]. Van Leussen and Nieuwenhuis [5] discussed the relevant soil mechanical parameters in 1984. Miedema [6] 1987 uses the average deformation rate as stated by van Os [12] 1977 but instead of inserting this in the Biot equation; the average deformation rate is modeled as a boundary condition in the shear zone. Although the cutting process is not solely dependent upon the phenomenon dilatancy, the above mentioned research showed that for cutting velocities in a range from 0.5 to 5 m/sec the cutting process is dominated by the phenomenon dilatancy, so the contributions of gravitational, cohesive, adhesive and inertial forces can be neglected, thus the cutting equations can be simplified to (Miedema, 1987 [6]):

The non-cavitating cutting process:

$$F_h = \frac{c_1 \cdot \rho_w \cdot g \cdot v_c \cdot h_i^2 \cdot b \cdot e}{k_m} \tag{1}$$

$$F_v = \frac{c_2 \cdot \rho_w \cdot g \cdot v_c \cdot h_i^2 \cdot b \cdot e}{k_m} \tag{2}$$

The cavitating cutting process:

$$F_h = d_1 \cdot \rho_w \cdot g \cdot (z+10) \cdot h_i \cdot b \tag{3}$$

$$F_v = d_2 \cdot \rho_w \cdot g \cdot (z+10) \cdot h_i \cdot b \tag{4}$$

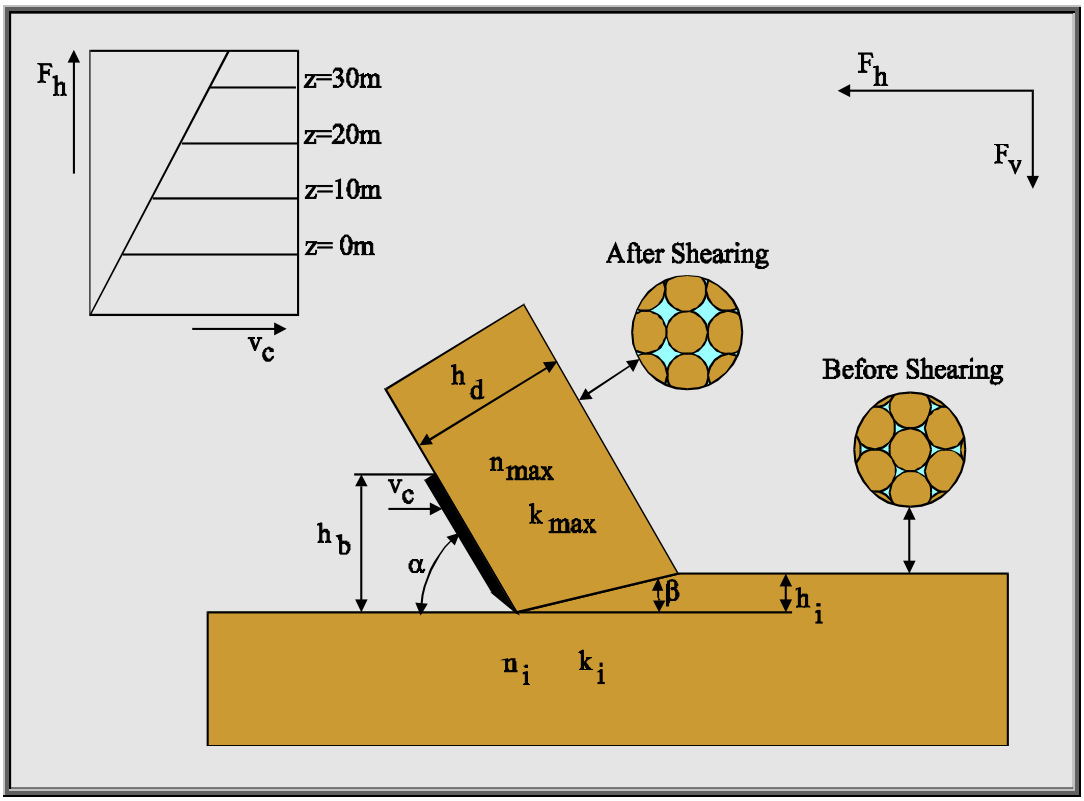

Fig. 5: The occurrence of dilatation when cutting water saturated sand.

## SPECIFIC ENERGY.

To determine the production of excavating elements as a function of the SPT value of the soil, the specific energy method is used. The specific energy is the amount of energy (work) required for the excavation of one cubic meter of in-situ soil. The dimension of specific energy is kNm/m$^3$ or kPa. The specific energy depends on the type of soil (soil mechanical parameters), on the geometry of the excavating element (dredging wheel, crown cutter, etc.) and on the operational parameters (haulage velocity or trail velocity, revolutions, face geometry, etc). Beside the above, the effective specific energy will be influenced by other phenomena such as spill, wear and the bulldozer effect. The maximum production can also be limited by the hydraulic system. The production can be derived from the specific energy by dividing the available power by the specific energy.

$$Q = P_a / E_s \qquad (5)$$

An accurate calculation of the specific energy and thus the production can be carried out only when all off the parameters influencing the cutting process are known. If an estimate has to be made of the specific energy and the production, based on the SPT value only, a number of assumptions will have to be made and a number of approximations will have to be applied. These assumptions and approximations will

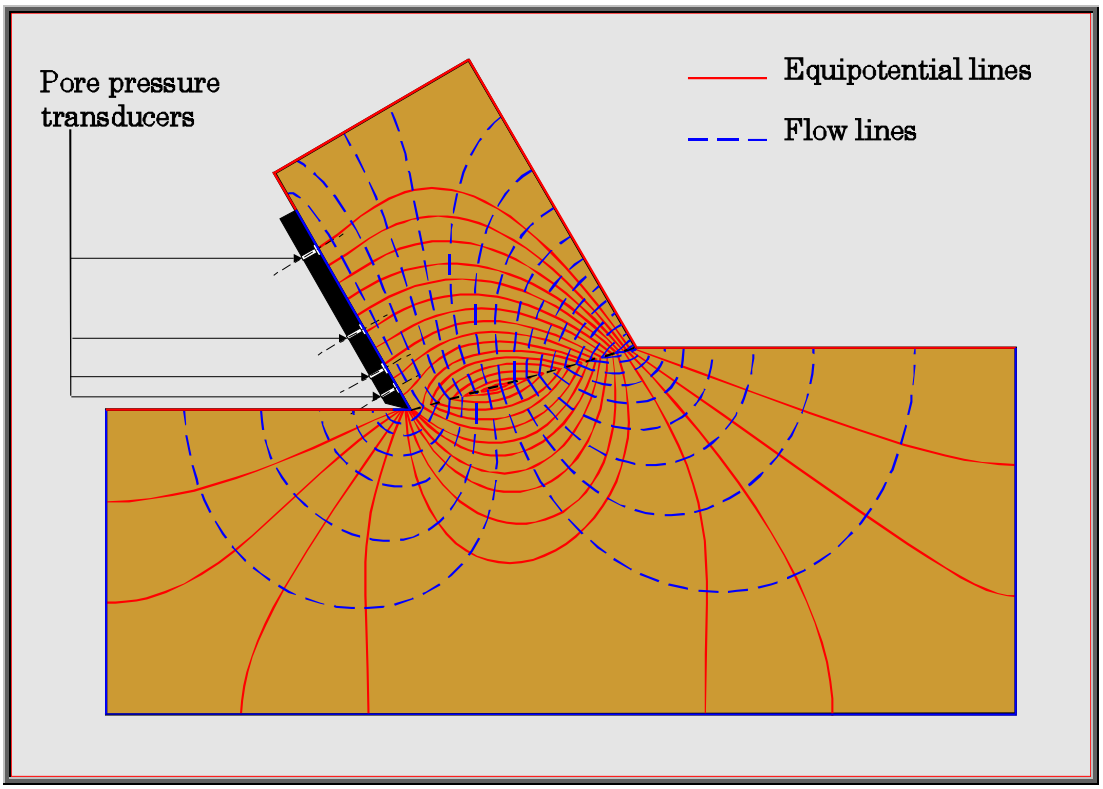

Fig. 6: Equipotential and flow lines, showing the pore pressures.

maximize the specific energy and thus minimize the production. In other words, the specific energy as calculated in this paper is an upper limit, whilst the calculated production is a lower limit. Wear, spill and limitations such as the bulldozer effect are not taken into consideration. Once the specific energy and the production per 100 kW are known, the production, giving an available power, can be calculated. This production can be either realistic, meaning that the bulldozer effect will not occur, or not realistic meaning that this effect will occur. In the last case, the maximum production will have to be calculated from the limitations caused by the bulldozer effect. From the maximum production derived, the maximum swing velocity, giving a certain bank height and step size, can be determined. The type of cutting process is determined by the soil mechanical properties of the soil to be dredged, the geometry of the excavating element and the operational parameters.

## SPECIFIC ENERGY AND PRODUCTION IN SAND.

As discussed previously, the cutting process in sand can be distinguished in a non-cavitating and a cavitating process, in which the cavitating process can be considered to be an upper limit to the cutting forces. Assuming that during an SPT test in water-saturated sand, the cavitating process will occur, because of the shock wise behaviour during the SPT test, the SPT test will give information about the cavitating cutting process. Whether, in practice, the cavitating cutting process will occur, depends on the soil mechanical parameters, the geometry of the cutting process and the operational parameters. The cavitating process gives an upper limit to the forces, power and thus the

specific energy and a lower limit to the production and will therefore be used as a starting point for the calculations.
For the specific energy of the cavitating cutting process, the following equation can be derived according to Miedema [6, page 148]:

$$E_s = \frac{F_h \cdot v_c}{h_i \cdot b \cdot v_c} = d_1 \cdot \rho_w \cdot g \cdot (z + 10) \qquad (6)$$

In Miedema [9], a derivation is given on the relation between de SPT value and the value of the only unknown in equation 6, the coefficient $d_1$.

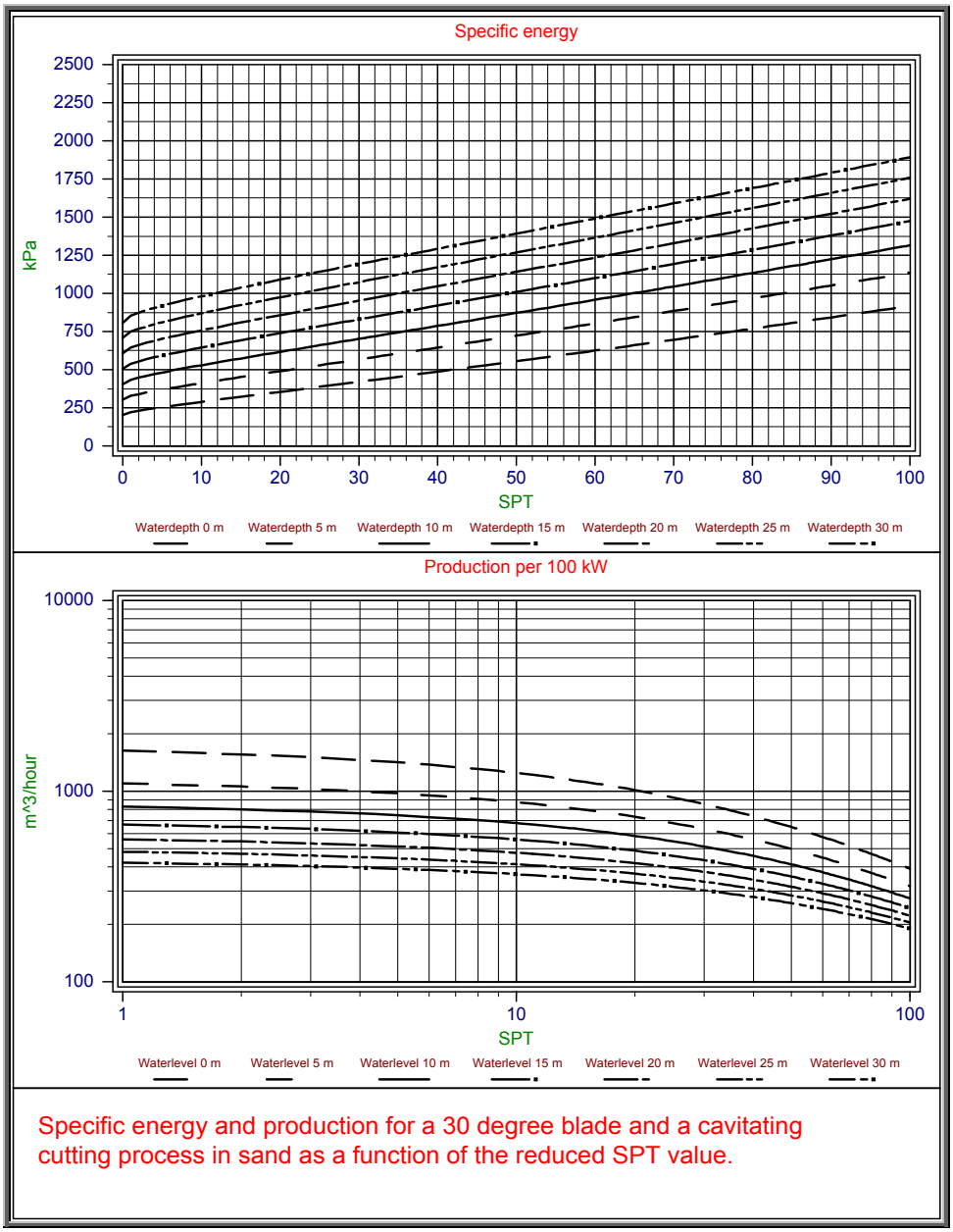


Fig. 7: The specific energy and maximum production.

With this relation, the maximum specific energy can be determined for a range of waterdepths as shown in figure 7. Once the maximum specific energy is known, the production can be determined given the available power. Figure 7 shows the production per 100 kW as a function of the maximum specific energy and the SPT value of the sand. These graphs are based on research in the Laboratory of Dredging Technology (T.U. Delft). Results of this research can be found in Miedema [6, 8 & 9]. Figure 8 shows a cross-section of the cutting rig in the laboratory.
The above decribes the limitations of the cutting process as a result of power limitations. There are two other important limitations, clogging and the bulldozer effect. Clogging occurs when the layer cut does not fit between two blades of the cutterhead. This deformed layer thickness depends on the swing velocity, the revolutions, the number of blades, and the cutting angle and depends on the type of sand through the angle of the shear plane.

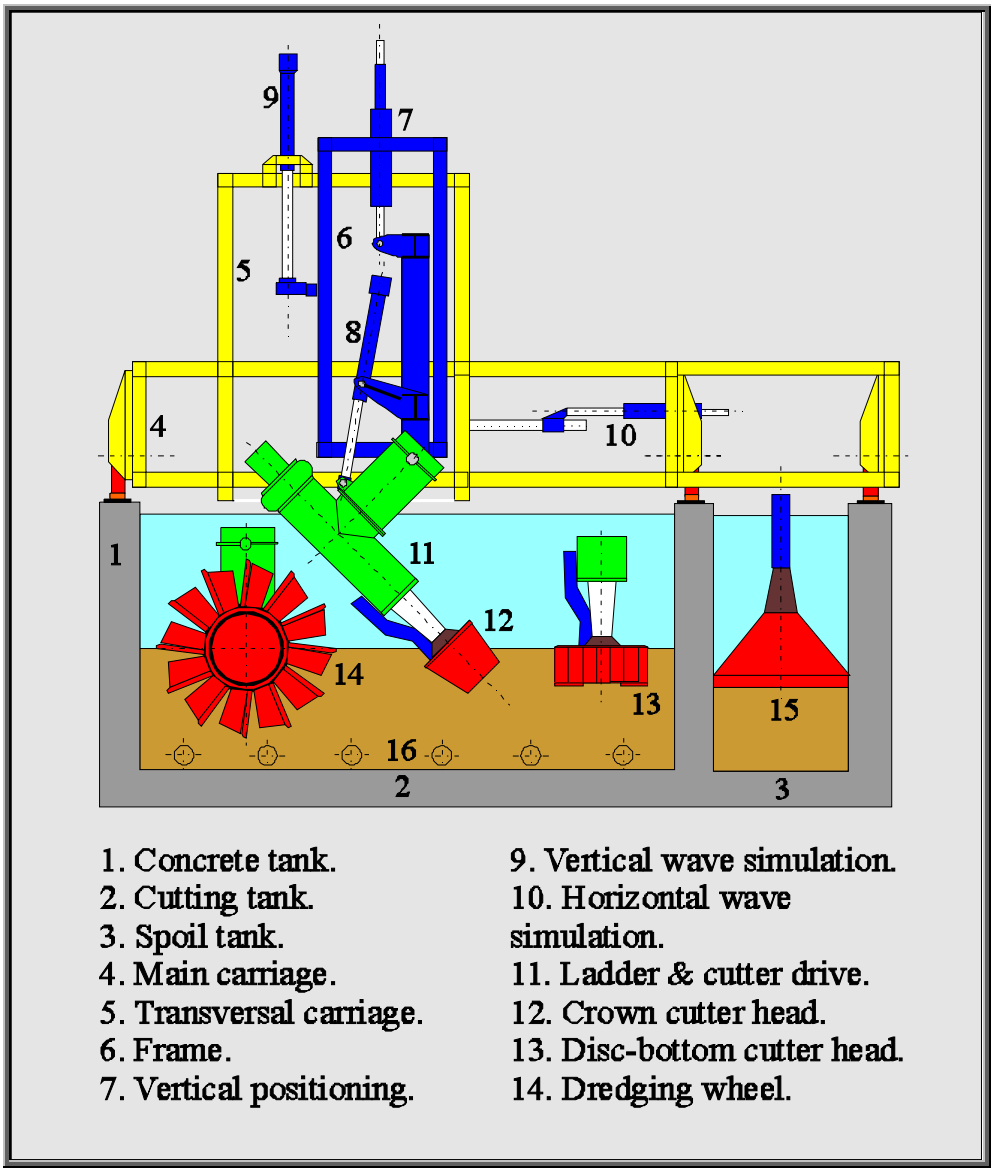

Fig. 8: A cross section of the Dredging Technology Laboratory (T.U. Delft).

The thickness of the deformed layer cut can be determined with:

$$h_{def} = \frac{v_s \cdot 60}{n_o \cdot p} \cdot \frac{\sin(\alpha+\beta)}{\sin(\beta)} \tag{7}$$

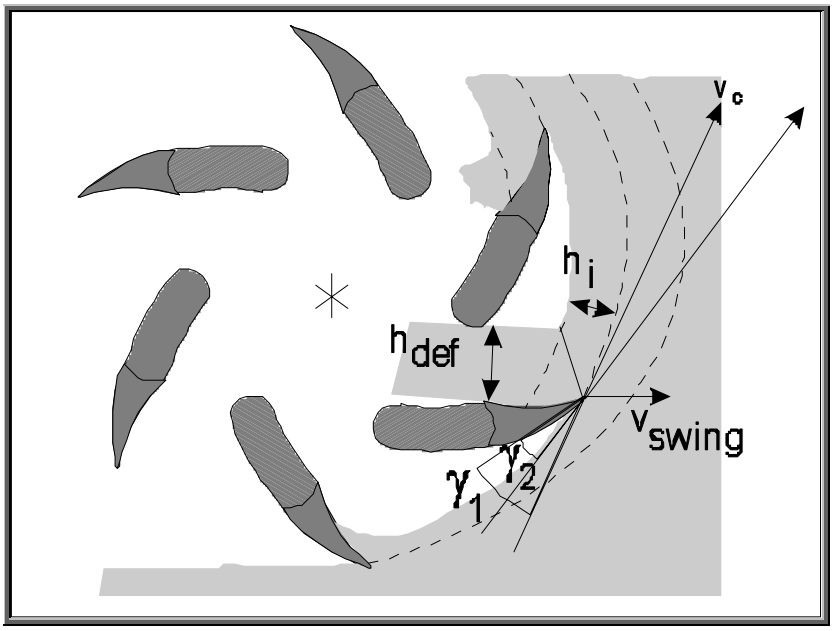


Fig. 9: The deformed layer thickness and the free running angle.

Figure 9 shows the deformed layer thickness. From this figure, it is obvious, that the throughput also depends strongly on the shape of the blades. The throughput can be defined as the shortest distance between the carrier line on the cutting edge of a blade and the back of the previous blade. When the deformed layer thickness does not fit anymore between two blades, the cutterhead becomes clogged first and then starts to bulldozer, because there is no way out for the sand. From equation 7, it is obvious that this will occur with a high swing velocity/revolutions ratio.

Another phenomenon that may cause the cutterhead to bulldozer is, when the sand hits the back of the blade of the cutterhead. Figure 9 shows the free running angle based on the circumferential velocity $\gamma_1$. Because of the swing velocity the actual free running angle $\gamma_2$ is smaller. When the value of the actual free running angle approaches zero, the sand will be pushed away by the back of the blade. This effect is determined by the free running angle, the circumferential velocity, the swing velocity and the direction of the circumferential velocity. One can see from figure 9 that this effect is at a maximum when the circumferential velocity is vertical.

Resuming it can be stated that clogging and bulldozing will limit the maximum cutting production at low SPT values, while the available power will limit the maximum production at low SPT values. The transition between the limiting factors depends on the geometry of the cutterhead, the power installed and on the operation parameters.

## INTRODUCTION TO HYDRAULIC TRANSPORT.

A multi pump/pipeline system consists of components with different dynamic behaviour. To model such a system, one should start with simple mathematical descriptions of the sub-systems, to be able to determine the sensitivity of the behaviour of the system to changes in one of the sub-systems. The following sub-systems can be distinguished:

- The pump drive
- The centrifugal pump
- The sand/water slurry in the pipeline
- Flow control (if used)

The system is limited by cavitation at the entrance of each pump on one hand and by sedimentation of the solids resulting in plugging of the pipeline on the other hand.The system is also limited by the power installed and the torque speed curve of each individual pump. Cavitation will occur at high line velocities and/or at high solids concentrations in the suction pipe of the pump considered. Sedimentation will occur at line velocities below the so called critical velocity. The critical velocity depends on the grain distribution and on the solids concentration. In between these two limitations a stable transportation process is required. A steady state process is possible only if the solids properties and the solids concentration are constant in time. In practice however this will never be the case. Solids properties such as the grain size distribution will change as a function of time and place as will the solids concentration. The resistance of the slurry flow depends on the solids properties and concentration. If the total resistance of the slurry flow in a long pipeline is considered, changes of the solids properties and concentration at the suction mouth will result in slow changes of the total resistance, since only a small part of the pipeline is filled with the new slurry while most of the pipeline remains filled with the slurry that was already there, except from the slurry that has left the pipeline at the end. If the relatively short suction line is considered, this results in a much faster change of the vacuum at the inlet of the first pump.

The total head of a pump however, responds immediately to changes of the solids properties and concentration. If a sudden increase of the concentration is assumed, the total head of a pump will increase almost proportionally with the concentration. This will result in a higher flow velocity, but, because of the inertia of the slurry mass in the pipeline, the slurry mass will have to accelerate, so the flow velocity responds slowly on changes of the total head. The increase of the total head also causes an increase of the torque and power of the pump drive, resulting in a decrease of the pump drive revolutions and thus of the total head. Because of the inertia of pump and pump drive, there will not be an immediate response.

It is obvious that there is an interaction between all the different sub-systems. These interactions can be ranged from very slow to immediate. To be able to model the system, first the characteristic behaviour of the sub-systems should be known.

## THE PUMP DRIVE.

Pump drives used in dredging are diesel direct drives, diesel/electric drives and diesel/hydraulic drives. In this paper the diesel direct drive, as the most common arrangement, is considered.

At nominal operating speed, the maximum load coincides with the nominal full torque point. If the torque is less then the nominal full torque, the engine speed usually rises slightly as the torque decreases. This is the result of the control of the speed by the governor. The extent of this depends upon the type of governor fitted.
If the engine load increases above the full torque point, the speed decreases and the engine operates in the full fuel range. With most diesel engines the torque will increase slightly as the speed decreases, because of a slightly increasing efficiency of the fuel pumps. When the load increases further, insufficient air is available to produce complete combustion and the engine stalls. The torque drops rapidly and heavily polluted gasses are emitted. The smoke limit has been reached. The speed range between the full torque point and the smoke limit is often referred to as the constant torque range.
The torque/speed characteristic of the diesel engine can thus be approximated by a constant full torque upon the nominal operating speed, followed by a quick decrease of the torque in the governor range.

## THE CENTRIFUGAL PUMP.

The behaviour of centrifugal pumps can be described with the Euler impulse moment equation:

$$\Delta p_E = \rho_f \cdot u_o \cdot \left( u_o - \frac{Q \cdot \cot(\beta_o)}{2 \cdot \pi \cdot r_o} \right) - \rho_f \cdot u_i \cdot \left( u_i - \frac{Q \cdot \cot(\beta_i)}{2 \cdot \pi \cdot r_i} \right) \tag{8}$$

For a known pump this can be simplified to:

$$\Delta p_E = \rho_f \cdot \left( C_1 - C_2 \cdot Q \right) \tag{9}$$

Because of incongruity of impeller blades and flow, the finite number of blades, the blade thickness and the internal friction of the fluid, the Euler pressure $\Delta p_E$ has to be corrected with a factor **k**, with a value of about 0.8. This factor however does not influence the efficiency. The resulting equation has to be corrected for losses from frictional contact with the walls and deflection and diversion in the pump and a correction for inlet and impact losses. The pressure reduction for the frictional losses is:

$$\Delta p_{h.f.} = C_3 \cdot \rho_f \cdot Q^2 \tag{10}$$

For a given design flow $Q_d$ the impact losses can be described with:

$$\Delta p_{h.i.} = C_4 \cdot \rho_f \cdot \left( Q_d - Q \right)^2 \tag{11}$$

The total head of the pump as a function of the flow is now:

$$\Delta p_p = k \cdot \Delta p_E - \Delta p_{h.f.} - \Delta p_{h.i.} = \rho_f \cdot \left( k \cdot \left( C_1 - C_2 \cdot Q \right) - C_3 \cdot Q^2 - C_4 \cdot \left( Q_d - Q \right)^2 \right) \qquad (11)$$

Based on this theory, the characteristics of a pumps used is given in figures 10. The pump is limited by the constant torque behaviour of the corresponding diesel engine in the full fuel range.

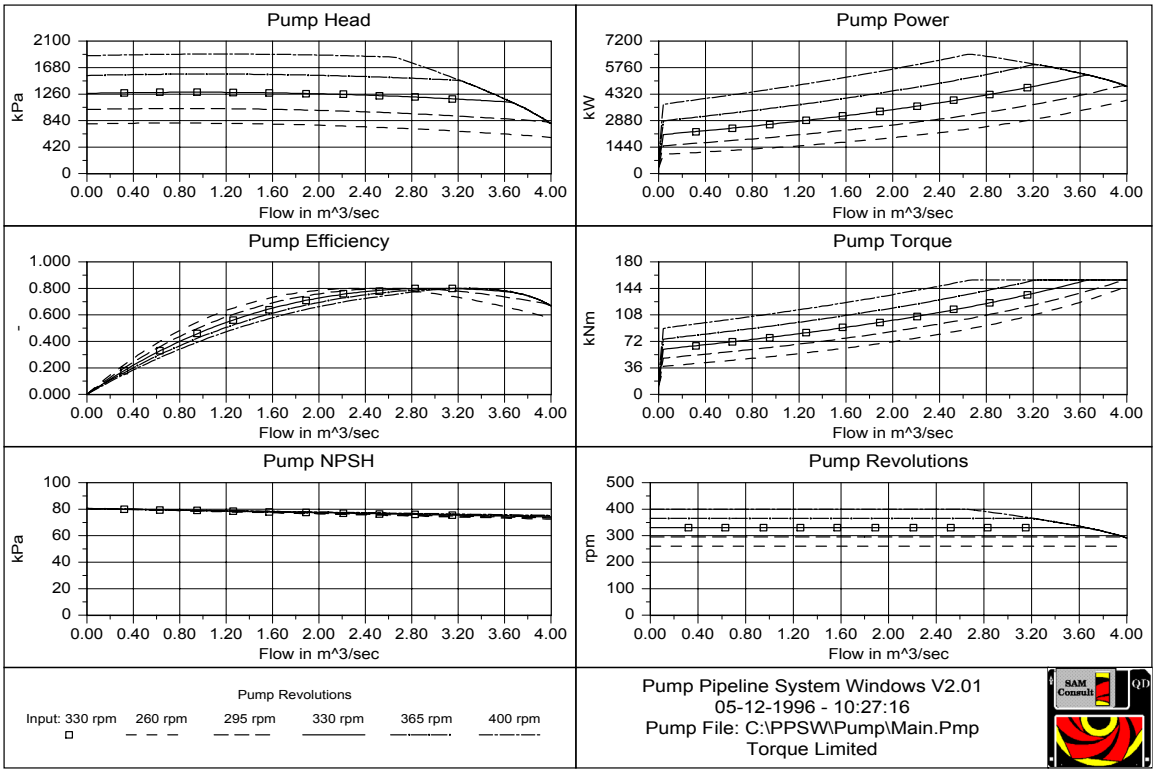


Fig. 10: The characteristics of the main pump and the booster pump.

Figures 10 gives the pump characteristics for clear water. If a mixture is pumped however, the pump head increases because of the mixture density and the pump efficiency decreases because a heterogeneous mixture is flowing through the pump. The decrease of the efficiency depends upon the average grain diameter, the impeller diameter and the solids concentration and can be determined with (according to Stepanoff):

$$\eta_m = \left( 1 - C_t \cdot \left( 0.466 + 0.4 \cdot \mathrm{Log10}\left( d_{50} \right) \right) / D \right) \qquad (12)$$

## PRESSURE LOSSES WITH HOMOGENEOUS WATER FLOW.

When clear water flows through the pipeline, the pressure loss can be determined with the well known Darcy-Weisbach equation:

$$\Delta p_w = \lambda \cdot \frac{L}{D} \cdot \frac{1}{2} \cdot \rho_w \cdot c^2 \qquad (13)$$

The value of the friction factor $\lambda$ depends on the Reynolds number:

$$\mathbf{Re} = \frac{\mathbf{c} \cdot \mathbf{D}}{\boldsymbol{\nu}} \tag{14}$$

## PRESSURE LOSSES WITH HETEROGENEOUS FLOW.

For the determination of the pressure losses of a heterogeneous flow many theories are available, like Durand/Condolios/Gibert, Fuhrboter, Jufin/Lopatin and Wilson. In this paper the Durand/Condolios/Gibert theory will be used, further referred to as the Durand theory. Durand assumes that the clear water resistance in a pipeline should be multiplied by a factor depending on the line speed, the grain size distribution and the concentration. Miedema, 1996 [11] added the inertial pressure to the equation.

$$\Delta \mathbf{p}_m = \Delta \mathbf{p}_w \cdot \left(1 + \Phi \cdot \mathbf{C}_t\right) + \sum_1^n \xi_n \cdot \tfrac{1}{2} \cdot \rho_m \cdot \mathbf{c}^2 + \rho_m \cdot \mathbf{g} \cdot \mathbf{H}_g + \rho_m \cdot \mathbf{L} \cdot \dot{\mathbf{c}} \tag{15}$$

In which:

$$\Phi = 180 \cdot \left( \frac{\mathbf{c}^2}{\mathbf{g} \cdot \mathbf{D}} \cdot \sqrt{\mathbf{C}_x} \right)^{-3/2} \tag{16}$$

and:

$$\mathbf{C}_x = \frac{\mathbf{g} \cdot \mathbf{d}}{\mathbf{v}^2} \tag{17}$$

The second term in the right hand side gives the resistance of all bendings, valves, etc. The third term gives the resistance of the geodetic height and the fourth term the inertial resistance. Since $\mathbf{Fr}_{fl} = \frac{\mathbf{c}}{\sqrt{\mathbf{g} \cdot \mathbf{D}_p}}$ is the Froude number for the flow in the pipeline and $\mathbf{Fr}_{gr} = \frac{\mathbf{v}}{\sqrt{\mathbf{g} \cdot \mathbf{d}}}$ is the Froude number for the settling process of a grain, equation 16 can also be written as:

$$\Phi = 176 \cdot \mathbf{Fr}_{fl}^{-3} \cdot \mathbf{Fr}_{gr}^{1.5} \tag{18}$$

In normal sands, there is not only one graindiameter, but a grain size distribution has to be considered. The Froude number for a grain size distribution can be determined by integrating the Froude number as a function of the probability according to:

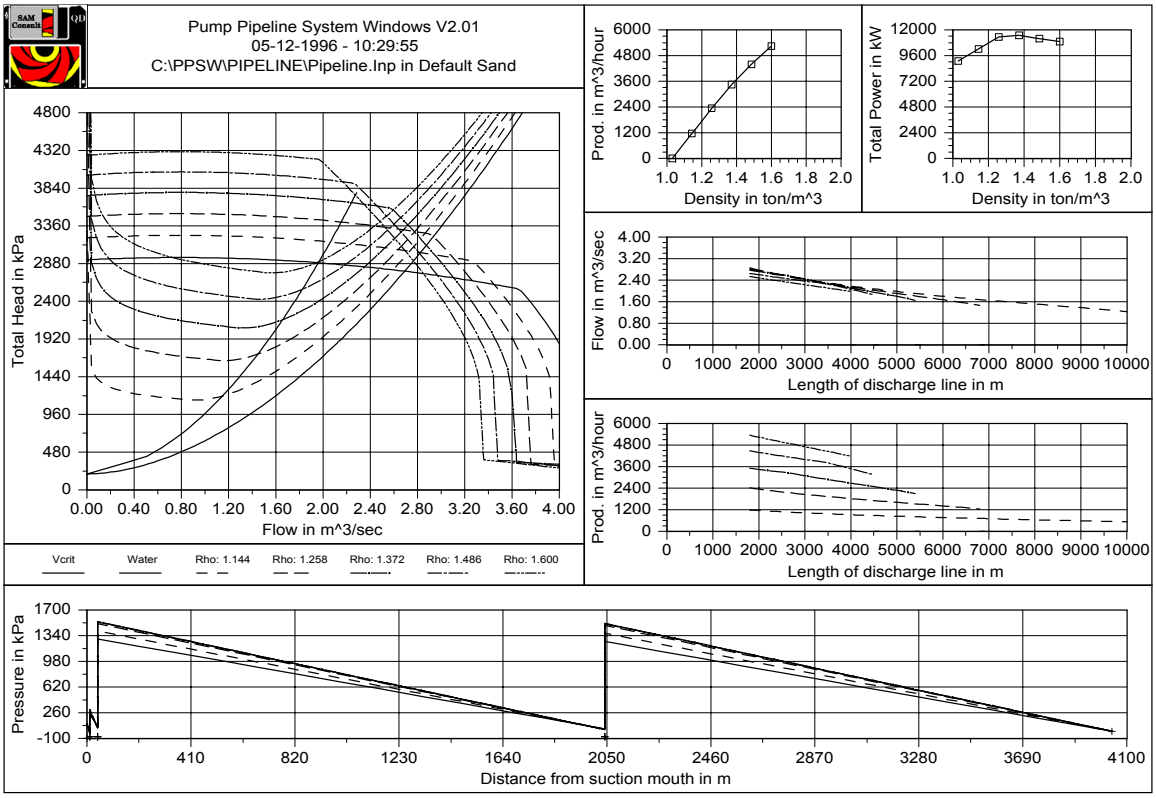

Fig. 11: Characteristics of the pump/pipeline system.

$$\mathbf{Fr_{gr}} = \frac{\mathbf{1}}{\int_{\mathbf{0}}^{\mathbf{1}} \frac{\sqrt{\mathbf{g \cdot d}}}{\mathbf{v}} \mathbf{dp}} \tag{19}$$

When the flow decreases, there will be a moment where sedimentation of the grains starts to occur. The corresponding line speed is called the critical velocity. Although in literature researchers do not agree on the formulation of the critical velocity, the value of the critical velocity is often derived by differentiating equation 15 with respect to the line speed **c** and taking the value of **c** where the derivative equals zero. This gives:

$$\mathbf{c_{cr}} = \sqrt{\frac{\mathbf{g \cdot D_p \cdot \left(90 \cdot C_t\right)^{2/3}}}{\sqrt{\mathbf{C_x}}}} \tag{20}$$

At line speeds less then the critical velocity sedimentation occurs and part of the cross-section of the pipe is filled with sand, resulting in a higher flow velocity above the sediment. Durand assumes an equilibrium between sedimentation and scour, resulting in a Froude number equal to the Froude number at the critical velocity.

$$Fr_{cr} = \frac{c_{cr}}{\sqrt{g \cdot D_p}} = \sqrt{\frac{\left(90 \cdot C_t\right)^{2/3}}{\sqrt{C_x}}} \qquad (21)$$

By using the hydraulic diameter concept, at lines speeds less then the critical velocity, the resistance can be determined.

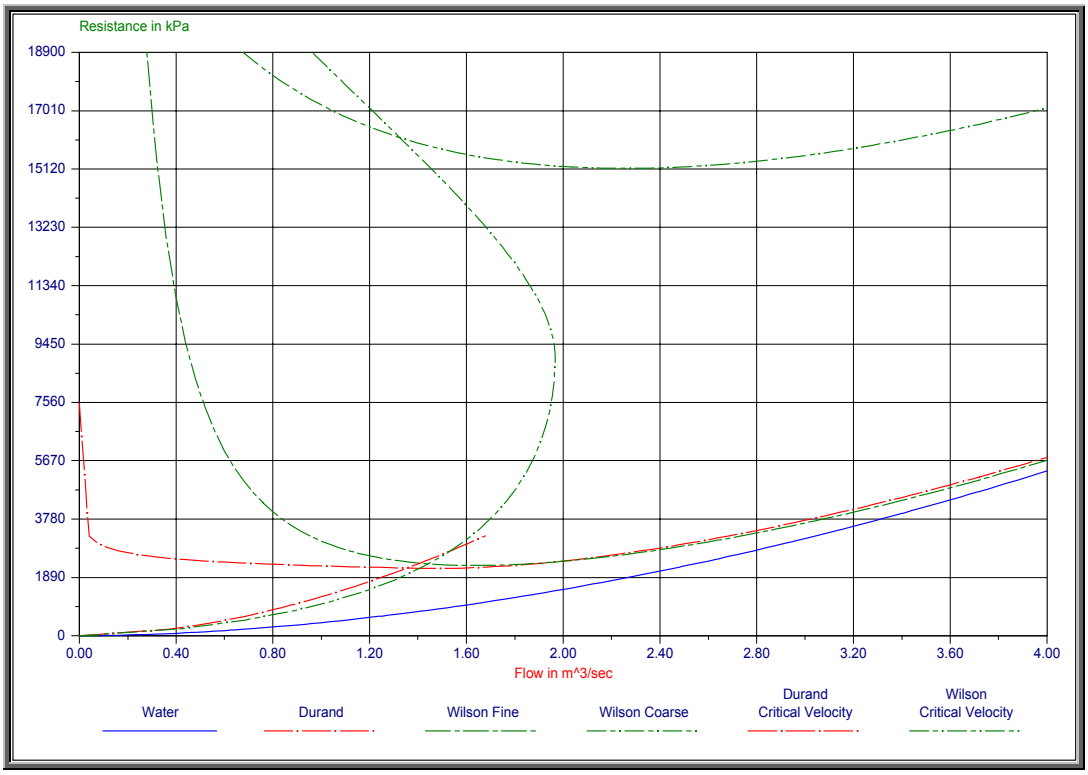


Fig. 12: A comparison between Durand and Wilson.

Figure 12 shows the water resistance, the mixture resistance and the critical velocity according to Durand [2] and Wilson [15] for a fine sand. Durand and Wilson match well in this case for fine sands, but for coarse sands they differ quite a lot.

## THE PUMP /PIPELINE SYSTEM DESCRIPTION.

In a steady state situation, the revolutions of the pumps are fixed, the line speed is constant and the solids properties and concentration are constant in the pipeline. The working point of the system is the intersection point of the pump head curve and the pipeline resistance curve. The pump curve is a summation of the head curves of each pump according to equation 11. The resistance curve is a summation of the resistances of the pipe segments and the geodetic head according to equation 15. Figure 11 shows this steady state situation for the system used in the case study at 6 densities ranging from clear water upto a density of 1.6 ton/m$^3$. In reality, the solids properties and concentration are not constant in time at the suction mouth. As a result of this, the solids properties and concentration are not constant as a function of the position in the pipeline.

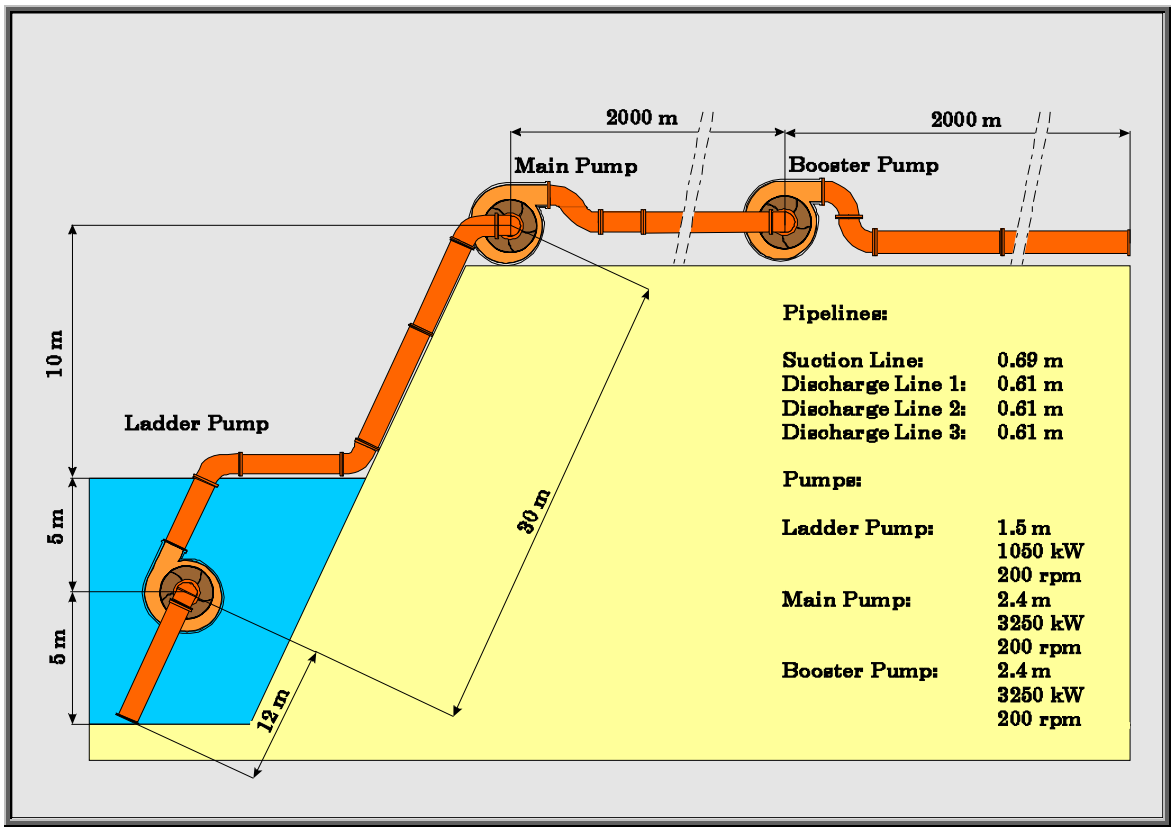

Fig. 13: The pump/pipeline layout as used in the case studies of Miedema [11].

To be able to know these properties as a function of the position in the pipeline, the pipeline must be divided into small segments. These segments move through the pipeline with the line speed. Each time step a new segment is added at the suction mouth, while part of the last segment leaves the pipeline. Because the line speed is not constant, the length of the segment added is not constant, but equals the line speed times the time step. For each segment the resistance is determined, so the resistance as a function of the position in the pipeline is known. This way also the vacuum and the discharge pressure can be determined for each pump. If vacuum results in cavitation of one of the pumps, the pump head is decreased by decreasing the pump density, depending on the time the pump is cavitating. The dynamic calculations are carried out in the time domain, because most of the equations used are non-linear. The time step used is about 1 second, depending on the speed of the PC and the other tasks Windows has to carry out.

Figure 14 shows cavitation as a limiting condition on the booster pump of the system described in figure 13. The simulations are described fully in Miedema [11]. The cavitation in this case is a result of a density wave.

## CONCLUSIONS.

In this paper, many limiting conditions for the operations of cutter suction dredgers are described. For the cutting process these are:

1. Power and torque limitations

2. A thick deformed layer cut, resulting in cloggingand the bulldozer effect
3. A negative free running angle, resulting in the bulldozer effect.

For the hydraulic transport process these are:
1. Sedimentation, resulting in clogging of the pipeline
2. Power and torque limitations, resulting in a decrease of the pump head, which can be used for a more stable process.
3. Cavitation, resulting in a fast pressure drop of the pump and a consequent decrease of the line velocity.

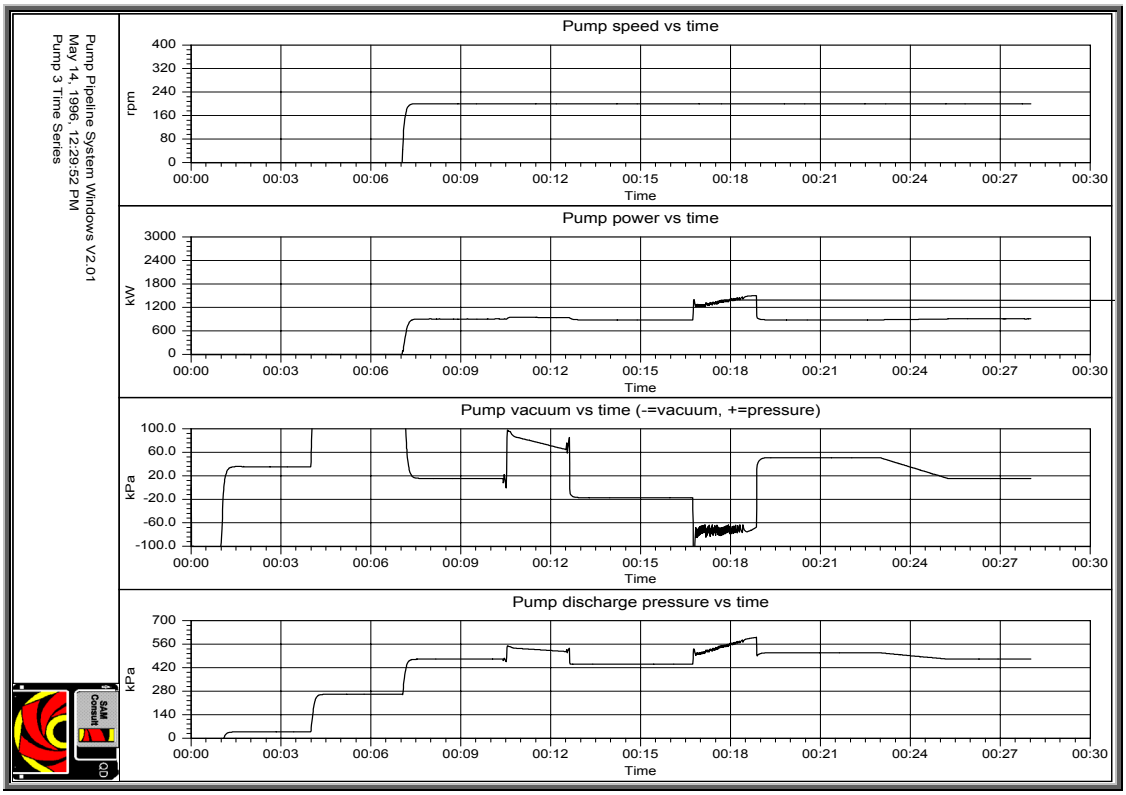

Fig. 14: Cavitation as a limiting condition on the booster pump.

Because of the dynamics of the two processes involved, it is hardly impossible to predict when one of the limits is reached, as would be for a stationary process. The only way to carry out predictions is to use a simulation program.
For a stationary situation the following rules can be applied:
Step 1: Determine the production curve according to figure 7.
Step 2: Determine the limits for the layer thickness and free running angle, based on swing velocity and revolutions of the cutterhead.
Step 3: Adjust figure 7 for the limiting conditions.
Step 4: Determine the critical velocity for the hydraulic system at the required density (figure 11) and for the sand properties.
Step 5: Determine the cavitation limits for each pump in the system.
Step 6: Adjust figure 7 for the hydraulic limits.
Step 7: Never excavate a production beyond the limits of the adjusted figure 7.

**LITERATURE.**


[ 1] Bree, S.E.M. de 1977, "Centrifugal Dredgepumps". IHC Holland 1977.

[ 2] Gibert, R., "Transport Hydraulique et Refoulement des Mixtures en Conduites".

[ 3] Hatamura, Y, & Chijiiwa, K., "Analyses of the mechanism of soil cutting".
1st report, Bulletin of the JSME, vol. 18, no. 120, June 1975.
2st report, Bulletin of the JSME, vol. 19, no. 131, May 1976.
3st report, Bulletin of the JSME, vol. 19, no. 139, November 1976.
4st report, Bulletin of the JSME, vol. 20, no. 139, January 1977.
5st report, Bulletin of the JSME, vol. 20, no. 141, March 1977.

[ 4] Huisman, L. 1995, "Sedimentation and Flotation". Lecture Notes, Delft University Of Technology 1973-1995.

[ 5] Leussen, W. van & Nieuwenhuis J.D., "Soil Mechanics Aspects of Dredging". Geotechnique 34 No.3, pp. 359-381, 1984.

[ 6] Miedema, S.A., "The Calculation of the Cutting Forces when Cutting Water Saturated Sand, Basical Theory and Applications for 3-Dimensional Blade Movements with Periodically Varying Velocities for in Dredging Usual Excavating Elements" (in Dutch). PhD thesis, Delft, 1987, the Netherlands.

[ 7] Miedema, S.A., "On the Cutting Forces in Saturated Sand of a Seagoing Cutter Suction Dredger". Proc. WODCON XII, Orlando, Florida, USA, April 1989. And Terra et Aqua No. 41, December 1989, Elseviers Scientific Publishers.

[ 8] Miedema, S.A., "On the Snow-Plough Effect when Cutting Water Saturated Sand with Inclined Straight Blades". ASCE Proc. Dredging 94, Orlando, Florida, USA, November 1994.

[ 9] Miedema, S.A., "Production Estimation Based on Cutting Theories for Cutting Water Saturated Sand". Proc. WODCON IV, November 1995, Amsterdam, The Netherlands 1995.

[10] Miedema, S.A. 1996, "Pump Pipeline System Windows V2.01". Software, Delft 1996.

[11] Miedema, S.A., "Modelling and Simulation of the Dynamic Behaviour of a Pump/Pipeline System". 17th Annual Meeting & Technical Conference of the Western Dredging Association. New Orleans, June 1996.

[12] Os, A.G. van, "Behaviour of Soil when Excavated Underwater". International Course Modern Dredging. June 1977, The Hague, The Netherlands.

[13] Os, A.G. van & Leussen, W. van, "Basic Research on Cutting Forces in Saturated Sand". Journal of Geotechnical Engineering, Vol. 113, No.12, December 1987.

[14] Verruijt, A., "Offshore Soil Mechanics". Delft University of Technology, 1985-1994.

[15] Wilson, K.C. & Addie, G.R. & Clift, R. 1992, "Slurry Transport Using Centrifugal Pumps". Elsevier Science Publishers Ltd. 1992.

## NOMENCLATURE.

Sand Cutting:

| | | |
|---|---|---|
| A | Adhesive force on blade | N |
| b | Width of blade | m |
| C | Cohesive force on the shear plane | N |
| $c_{1,2}$ | Coefficient non-cavitating cutting process | - |
| $d_{1,2}$ | Coefficient cavitating cutting process | - |
| e | Fractional volume increase | - |
| $E_s$ | Specific energy | kPa |
| $F_h$ | Horizontal cutting force (direction of cutting velocity) | N |
| $F_v$ | Vertical cutting force (perpendicular to cutting velocity) | m/s |
| G | Gravitational force resulting from weight | N |
| g | Gravitational constant | $m/s^2$ |
| $h_b$ | Height of blade | m |
| $h_i$ | Height of layer cut | m |
| I | Inertial force on the shear plane | m |
| $k_m$ | Mean permeability | m/s |
| $K_1$ | Resultant force on the shear plane | N |
| $K_2$ | Resultant force on the blade | N |
| n | Porosity | - |
| $n_o$ | Cutterhead revolutions | rpm |
| $N_1$ | Normal force on the shear plane | N |
| $N_2$ | Normal force on blade | N |
| p | Number of blades cutterhead | - |
| $P_a$ | Available power | kW |
| Q | Production | $m^3/s$ |
| $S_1$ | Shear force on the shear plane | N |
| $S_2$ | Shear force on blade | N |
| vc | Cutting velocity | m/s |
| vs | Swing velocity | m/s |
| $W_1$ | Water underpressure force on the shear plane | N |
| $W_2$ | Water underpressure force on blade | N |
| $W_3$ | Water underpressure force on the back of the blade | N |
| z | Waterdepth | m |
| $\alpha$ | Blade angle | Deg. |
| $\beta$ | Angle of shear plane | Deg. |
| $\delta$ | Soil/interface friction angle | Deg. |
| $\phi$ | Angle of internal friction | Deg. |
| $\gamma$ | Free running angle of blade | Deg. |
| $\rho_w$ | Water density | $Ton/m^3$ |

Hydraulic transport:

| | | |
|---|---|---|
| $c$ | Line speed | m/sec |
| $C_{1,2,3,4}$ | Coefficients | |
| $C_d$ | Drag coefficient | |
| $C_t$ | Transport concentration | - |
| $C_v$ | Volumetric concentration | - |
| $C_x$ | Drag coefficient | |
| $d$ | Grain diameter | m |
| $D$ | Impeller diameter | m |
| $D$ | Pipe diameter | m |
| $Fr$ | Froude number | - |
| $g$ | Gravitational constant | $m/sec^2$ |
| $H$ | Height | m |
| $I$ | Mass moment of inertia | $ton \cdot m^3$ |
| $k$ | Constant | - |
| $K_p$ | Proportionality constant | kNms/rad |
| $L$ | Length of pipeline | m |
| $n$ | Revolutions | rpm |
| $p$ | Pressure | kPa |
| $P$ | Power | kW |
| $Q$ | Flow | $m^3/sec$ |
| $r$ | Radius | m |
| $Re$ | Reynolds number | - |
| $T$ | Torque | kNm |
| $u$ | Tangetial velocity | m/sec |
| $v$ | Settling velocity grains | m/sec |
| $\alpha,\beta$ | Coefficients | |
| $\beta$ | Blade angle | rad |
| $\varepsilon$ | Wall roughness | m |
| $\varepsilon$ | Ratio | - |
| $\Phi$ | Durand coefficient | - |
| $\eta$ | Efficiency | - |
| $\boldsymbol{\varphi}$ | Rotation angle of centrifugal pump | rad |
| $\dot{\boldsymbol{\varphi}}$ | Angular velocity of centrifugal pump | rad/sec |
| $\ddot{\boldsymbol{\varphi}}$ | Angular acceleration of centrifugal pump | $rad/sec^2$ |
| $\lambda$ | Friction coefficient | - |
| $\nu$ | Kinematic viscosity | $m^2/sec$ |
| $\rho$ | Density | $ton/m^3$ |
| $\tau$ | Time constant | sec |
| $\xi$ | Friction coefficient | - |
| $\psi$ | Shape factor | |